considers the roughness-induced scattering of the incident light into surface plasmon modes, and subsequent decay of the surface plasmons by absorption or reradiation through further scattering. The model appears especially suited to the case of metal gratings[15] and to cases where the scattering of surface plasmons is weak.[16] We will show in the following paper that the model predicts the angular variation of the s- and p-scat-

tered light and the anomalous light quite well. In this approach, however, it is necessary to make assumptions about the strength of the coupling between surface plasmon and roughness, and it is difficult to incorporate absorption consistently into the model. The microscopic approach we have outlined above appears more intuitive, especially for the case of rough surfaces with short-wavelength variations.

*Research supported by the Advanced Research Projects Agency.

[1] H. Davis, Proc. Inst. Elec. (London) Engrs. **101**, 209 (1954); P. Bechman and A. Spizzichino, *The Scattering of Electromagnetic Waves from Rough Surfaces* (Pergamon, New York, 1963).

[2] V. Twersky, IRE Trans. Antennas Propagation AP-5, 81 (1957).

[3] D. W. Berreman, Phys. Rev. **163**, 855 (1967).

[4] U. Fano, J. Opt. Soc. Am. **31**, 213 (1941).

[5] E. A. Stern, in *Optical Properties and Electronic Structure of Metals and Alloys*, edited by F. Abeles (North-Holland, Amsterdam, 1966).

[6] H. E. Bennett and J. O. Porteus, J. Opt. Soc. Am. **51**, 123 (1969).

[7] P. Dobberstein *et al.*, in Proceedings of the Second International Vacuum Ultraviolet Conference, Gatlinsburg, Tennessee, 1968 (unpublished); J. L. Stanford *et al.*, *ibid.*; S. E. Schnatterly, *ibid.*; also, S. N. Jasper-

son and S. E. Schnatterly, Phys. Rev. **188**, 759 (1969).

[8] O. Hunderi and D. Beaglehole, Phys. Letters 29A, 335 (1969); O. Hunderi and D. Beaglehole, Optics Commun. **1**, 101 (1969).

[9] H. E. Bennett, J. M. Bennett, E. J. Ashley, and R. J. Motyka, Phys. Rev. **165**, 755 (1968).

[10] D. Beaglehole, Appl. Opt. **7**, 2218 (1968).

[11] $dR/d\epsilon_2 > 0$ if $\epsilon_2 > (1 - 2\epsilon_1 + 3\epsilon_1^2)^{1/2}$, which is true for all the noble metals in their interband region.

[12] G. Mie, Ann. Phys. (N. Y.) **25**, 377 (1908).

[13] H. C. van de Hulst, *Light Scattering by Small Particles* (Wiley, New York, 1957).

[14] W. Steinmann, Phys. Status Solidi **28**, 437 (1968).

[15] Y. Y. Teng and E. A. Stern, Phys. Rev. Letters **19**, 511 (1967); R. H. Ritchie, E. T. Arakawa, J. J. Cowan, and R. N. Hamm, *ibid.* **21**, 1530 (1968).

[16] R. E. Wilems and R. H. Ritchie, Phys. Rev. Letters **19**, 1325 (1967); P. A. Fedders, Phys. Rev. **165**, 580 (1968).

Study of the Interaction of Light with Rough Metal Surfaces. II. Theory*

O. Hunderi and D. Beaglehole

Department of Physics and Astronomy, University of Maryland, College Park, Maryland 20742
(Received 23 September 1969)

In the preceding paper we described the measurements of the scattering, reflectivity, and transmission of light by metals whose surfaces were rough on a microscopic scale. In this paper we develop further the two theoretical approaches outlined in that paper. The first approach considers the radiation from surface currents modulated by the surface roughness. The second approach considers a model surface for which the reflection properties can be solved exactly, the model consisting of metal spheres located above a smooth metal surface. The two approaches demonstrate all the physical phenomena reported in the preceding experimental paper.

I. INTRODUCTION

The optical properties of the various rough surfaces we investigated in the preceding paper were surprisingly similar, depending mainly upon whether we were in a metallic region, a dielectric region, or a damped metallic region. However, none of the theories referred to in that paper gave

a satisfactory description of their properties.

In this paper, we develop two different approaches to the problem of absorption and scattering by rough metal surfaces. The first approach considers the radiation from surface currents induced by the incident light. The surface currents are taken to be of two parts: the usual polarization currents of a smooth surface now modulated by the roughness,

and extra surface-plasmon currents. We use the approach first initiated by Stern,[1] who calculated the radiation from the roughness modulated transverse-plasmon currents in a thin film. We have solved the problem for polarization and plasmon currents running parallel to the surface. This approach predicts very well the observed vector dependence of the background scattered light and the anomalous surface-plasmon radiation.

The second approach calculates the reflectance of a model surface consisting of spheres located just above a smooth metal surface. This is not as realistic a model as that of Berreman,[2] who considered hemispheres located on an otherwise smooth surface, but it has the important advantage that it can be solved exactly, and thus shows up the limitations of the earlier calculations. Twersky[3] calculated a similar model only for an infinite conductivity surface. Berreman calculated only to first order in the parameter $x = 2\pi a/\lambda$, with a the hemisphere radius, and in first order one retains only the dipole absorption effects. As we described in the previous paper, a simple consideration of spheres shows that higher-order radiation effects will be important for the roughness dimensions of our experiments.

II. RADIATION BY SURFACE CURRENTS

A. s- and p-Scattered Light

Electromagnetic fields in the presence of metallic boundaries give rise to induced surface charges and surface currents, and these are the origin of the reflected fields. For instance, when a plane wave is incident upon a flat metal surface, currents are set up in the skin depth having the same wave vector along the surface as the incident wave. The radiation from these currents must have the same component of wave vector in the surface in order to match the boundary conditions on the electric and magnetic fields. As a consequence radiation is only found in the specular direction.

When the surface is rough, the currents have normal as well as tangential wave vectors and the wave vector along the surface is modulated by the height variations. It is convenient to Fourier-analyze the height variation into components of different wavelengths, and the currents are then modulated along the surface with these periodicities. In order to find their radiation pattern one should integrate the appropriate Green's function over the actual volume in which the currents exist. As an approximation, we will consider the radiation from currents on a mean surface, their amplitudes modulated with the surface periodicity.

Well away from the resonance regions we need consider only the polarization currents. These are

responsible for the scattering in the dielectric region and for the background scattering for wavelengths much larger than λ_{sp} (see the preceding paper). To calculate the angular distribution of the radiation from these currents we proceed as follows. We write for the current

$$\vec{j}(\vec{r}) = \sum_{\vec{K}} \vec{j}_{\vec{K}} \, e^{\,i\vec{K}\cdot\vec{r}} \ .$$

As shown in the Appendix, the scattered intensity per unit solid angle per unit area from the component $\vec{j}_{\vec{K}} \, e^{\,i\vec{K}\cdot\vec{r}}$ is

$$\frac{dI}{d\Omega} = \frac{c}{8\pi} k^4 \cos^2\theta \, |\hat{n} \times \vec{A}_{\vec{K}}|^2 \ ,$$

where $\hat{n}$ is a unit vector in the radiation direction at an angle θ from the normal and $k = \omega/c$; since the radiation is found at angle θ, $|\vec{K}|$ must equal $(\omega/c)\sin\theta$. The strength of the radiation is proportional to the square of the vector potential $\vec{A}_{\vec{K}}$ of the fields associated with this current, and expressions for the s and p components of $\vec{A}_{\vec{K}}$ are derived in the Appendix. $|\vec{A}_{\vec{K}}|^2$ is proportional to $|\vec{j}_{\vec{K}}|^2$, where

$$|\vec{j}_{\vec{K}}|^2 = \frac{1}{(2\pi)^4} \int \int \vec{j}(\vec{r}) \cdot \vec{j}(\vec{r}')\, e^{\,i\vec{K}\cdot(\vec{r}-\vec{r}')} \, d\vec{r}\, d\vec{r}' \ .$$

The scattered intensity is thus determined by the correlation between the currents at two points in the surface. The latter can be written in terms of a current autocorrelation function $g(\vec{\zeta})$ defined by the expression

$$g(\vec{\zeta}) = \int_s \vec{j}(\vec{r}) \cdot \vec{j}(\vec{r}-\vec{\zeta})\, d\vec{r} \ .$$

$\vec{\zeta}$ is a length along the surface. $|\vec{j}_{\vec{K}}|^2$ is thus given by

$$|\vec{j}_{\vec{K}}|^2 = \frac{1}{(2\pi)^4} \int g(\vec{\zeta})\, e^{\,i\vec{K}\cdot\vec{\zeta}} \, d\vec{\zeta} \ .$$

If the currents are completely random on the surface, $g(\vec{\zeta})$ equals zero except for $\vec{\zeta} = 0$. If the currents are correlated over a distance a, $g(\vec{\zeta})$ falls to zero for ζ greater than a. Since $g(\vec{\zeta})$ is never known exactly for any particular surface, it is usually assumed to have a Gaussian distribution:

$$g(\vec{\zeta}) = I_0^2\, e^{-\zeta^2/a^2} \ .$$

The expression for the radiation in fact is completely general, valid for any kind of modulation — height, density fluctuations, etc. I_0^2 measures the strength of modulation. For the case of a rough surface, we can estimate the parameters determining I_0. The scattered radiation comes from currents flowing in the bumps of the surface (Fig. 1) and the vector potential is given by a volume integral of the current density in the bump, and thus is proportional to the volume of the bump δa^2. If N is the number of bumps per unit area, $|\vec{A}_{\vec{K}}|^2$ is
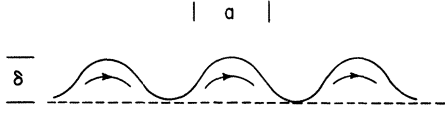
FIG. 1. Schematic current distribution on a rough surface.

proportional to $N\delta^2 a^4$ or $(\delta^2 a^2)$ (Na^2). Na^2 is a factor of order unity. I_0^2 is thus proportional to $\delta^2 a^2$.

Finally, the current in the metal is related to the incident electric field

$$\vec{j}_R = \sigma \vec{E}_t = \sigma t \vec{E}_0 \ .$$

$\vec{E}_t$ and $\vec{E}_0$ are the fields in the metal and outside, respectively, t is the transmission of the boundary, and σ is the metal's conductivity.

To obtain the total intensity reaching the detector we sum over the appropriate range of wave vectors; dividing by the incident intensity and the smooth-surface reflectivity, we obtain the following expressions for the fractional scattered light:

s-polarized light:

$$\frac{1}{R_s}\frac{dR_{sc\,\shortparallel}}{d\Omega} = \beta\,\delta^2 a^2 \left(\frac{\omega}{c}\right)^4 \left|1 + \sqrt{\epsilon}\right|^2$$

$$\times \left|\frac{\cos\theta}{(\epsilon - \sin^2\theta)^{1/2} + \cos\theta}\right|^2 e^{-(\pi^2 a^2/\lambda^2)\sin^2\theta} \ ;$$
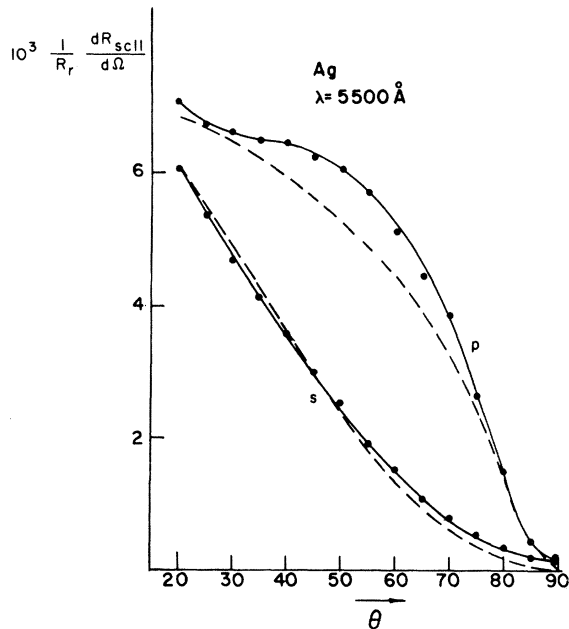

FIG. 2. Solid line: angular distribution of the relative scattered intensity measured with analyzer and polarizer parallel; dashed line: theoretical prediction with $a = 1100$ Å.
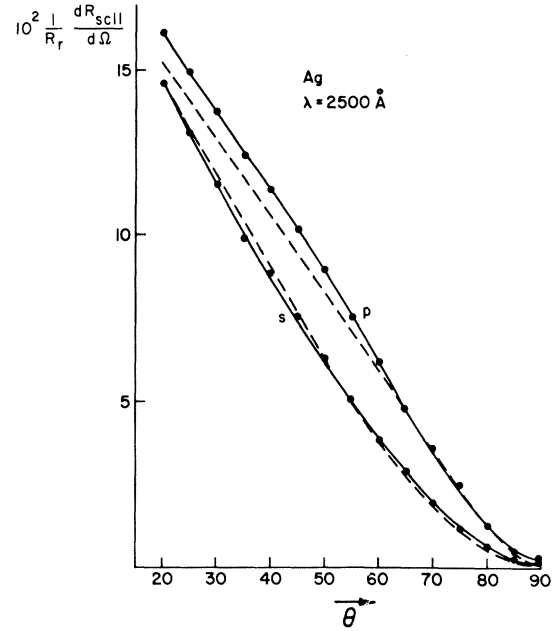

FIG. 3. Solid line: angular distribution of the relative scattered intensity measured with analyzer and polarizer parallel; dashed line: theoretical prediction with $a = 630$ Å.

p-polarized light:

$$\frac{1}{R_p}\frac{dR_{sc\,\shortparallel}}{d\Omega} = \beta\,\delta^2 a^2 \left(\frac{\omega}{c}\right)^4 \left|1 + \sqrt{\epsilon}\right|^2$$

$$\times \left|\frac{(\epsilon - \sin^2\theta)^{1/2}}{(\epsilon - \sin^2\theta)^{1/2} + \epsilon\cos\theta}\right|^2 \cos^2\theta \ e^{-(\pi^2 a^2/\lambda^2)\sin^2\theta} \ .$$

β is a numerical factor of the order 1.

The predictions of this theory for s- and p-polarized light are shown in Figs. 2 and 3, where we compare with the experimental angular distribution of the scattered light. The shape of the curves is reproduced remarkably well for both polarizations of incident light; it is seen that the anomalous p-polarized radiation is missing from the theory. The wavelength variation is not so good — it is necessary to choose different values for a for each wavelength. This may be a limitation of the theory, or quite possibly the autocorrelation function for these experimental surfaces may not be of the assumed Gaussian distribution form. Integrating the scattered light over all angles we found the total scattering due to these polarization currents. The result is shown in Fig. 4 for silver plotted on a ln-ln scale. The slope -3.2 is somewhat smaller than the experimental -4.5. Similar slopes are calculated for gold and copper, which are in better agreement with experiment for these metals. There are no resonances in this scattered light in the region of small negative ϵ.
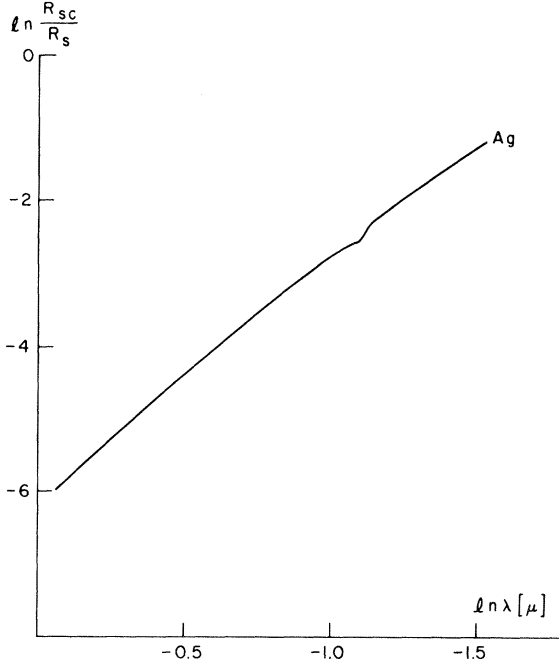
FIG. 4. Total relative scattering plotted on a ln-ln scale, calculated using the dielectric constant of bulk silver.

The approach here is in many ways similar to the scalar scattering theory,[4] but with the vector properties and finite conductivity properly taken into account. The approach appears to be a very good generalization of the scalar scattering theory.

B. Surface-Plasmon Anomalies

In the resonance region, the surface currents have an additional contribution coming from surface plasmons. On a smooth surface, the surface plasmons have a wave vector given by the dispersion relation $k_p^2 = (\omega/c)^2 |\epsilon|/(|\epsilon| -1)$, which is always greater than ω/c, so that they do not contribute to the interaction with external plane waves. But on a rough surface the wave vector of the incident light may be modulated to match $\vec{k}_p$, exciting surface plasmons, and the surface plasmons themselves may be modulated so that they have radiative components.

In the preceding paper, we observed extra contributions to the scattered light in the region below $\epsilon = -1$, which we associated with radiation from these surface-plasmon currents. The anomaly was always p polarized, for both s- and p-incident light, peaking between 50° and 60° and having a maximum intensity just below λ_{sp}. The theory of Sec. II A can be simply extended to include the surface-plasmon currents. There are two differences with Sec. II A. The first is that in this case k_p, which is large on a smooth surface, is reduced by the

modulation to give a radiative component. This modifies the angular variation of the radiated light. The second involves the polarization properties. The anomaly was observed to be always p polarized, even for s-incident light. Since the plasmon E field is mainly longitudinal (the ratio of longitudinal component to normal component being $\sqrt{|\epsilon|}$), the radiation must be due to surface-plasmon currents in the p direction. Thus a rotation of the polarization vector must occur during the interaction process. In Sec. II A the scattered light maintained its original polarization.

We picture the process as follows. The surface modulation of the normally incident light generates plasmon currents propagating in all directions with a strength depending upon $\vec{e}_{\vec{k}} \cdot \vec{e}_{\vec{k}_p}^*$; $\vec{e}_{\vec{k}}$ and $\vec{e}_{\vec{k}_p}$ are the polarization vectors of the incident light and of the plasmons, respectively. This surface plasmon will itself be modulated by the surface roughness and have a radiative component in the p direction. The anomalous radiation is due to this component. We find the angular distribution of this radiation, using the fields derived in the Appendix associated with currents of the appropriate polarization.

The ground state of a plasmon on a rough surface is no longer the harmonic wave with wave vector $\vec{k}_p$, but through modulation has components $\vec{k}_p + \vec{K}$. We write the wave function

$$\psi = \vec{e}_{\vec{k}_p}(\vec{e}_{\vec{k}_p}^* \cdot \vec{e}_{\vec{k}})e^{i\vec{k}_p \cdot \vec{r}} + \sum_{\vec{K}} \vec{e}_{\vec{k}_p + \vec{K}} \, a_{\vec{k}_p + \vec{K}} \cdot e^{i(\vec{k}_p + \vec{K}) \cdot \vec{r}}.$$

If we represent the modulation by a scattering interaction with a potential $V(r)$ [its Fourier transform is $V(\vec{K})$] which depends upon the local surface roughness, the coefficients $a_{\vec{k}_p + \vec{K}}$ are given by

$$|a_{\vec{k}_p + \vec{K}}|^2 = \frac{(\vec{e}_{\vec{k}_p}^* \cdot \vec{e}_{\vec{k}})^2(\vec{e}_{\vec{k}_p + \vec{K}}^* \cdot \vec{e}_{\vec{k}_p})^2 |V(\vec{K})|^2}{(\omega_{\vec{k}_p} - \omega_{\vec{k}_p + \vec{K}})^2 + \Gamma^2}.$$

Assuming $V(\vec{r})$ is proportional to the same surface roughness fluctuations as of Sec. II A, $|V(\vec{K})|^2$ becomes proportional to the Fourier transform of the autocorrelation function:

$$|V(\vec{K})|^2 \propto F(\vec{K}) = \int g(\vec{\xi})e^{i\vec{K} \cdot \vec{\xi}}d\vec{\xi} \quad .$$

The radiation from the component $a_{\vec{k}_p + \vec{K}}$ of the plasmon wave function we take to be equal to the classical radiation from a current

$$\vec{j} \propto \sigma a_{\vec{k}_p + \vec{K}} \, \vec{e}_{\vec{k}_p + \vec{K}} \cdot e^{i(\vec{k}_p + \vec{K}) \cdot \vec{r}}$$

on a smooth surface.

Fitting these terms together as we did in Sec. II A using the appropriate vector potential derived in the Appendix, we obtain the following expressions for the radiation from excited surface plasmons[5]:

$$\frac{dR_{sp}}{d\Omega} = \beta \frac{c}{8\pi} E_{sp}{}^2 a^2 \delta^2 \left(\frac{\omega}{c}\right)^4 \frac{[\,(\sigma_\shortparallel/\omega)(|\epsilon - \sin^2\theta|)^{1/2} - \sigma_\perp \sin\theta/\omega(|\epsilon_{\vec{K}'}|)^{1/2}]^2}{|(\epsilon - \sin^2\theta)^{1/2} + \epsilon\cos\theta|^2} \cos^2\theta P,$$

where
$$P = \left[\left(1 + \frac{1}{|\epsilon|}\right)\left(1 + \frac{1}{|\epsilon_{\vec{K}'}|}\right)\right]^{-1}\int_{-\pi/2}^{\pi/2} d\phi \,\cos^2\phi \left(\sin\phi + \frac{1}{(\epsilon\epsilon_{\vec{K}'})^{1/2}}\right)^2 \frac{\omega_{sp}^2}{(\omega_{\vec{K}_p} - \omega_{\vec{K}'})^2 + \Gamma^2} F(\vec{K}),$$

$\epsilon \equiv \epsilon(\omega_{\vec{K}_p})$, $\epsilon_{\vec{K}'} \equiv \epsilon(\omega_{\vec{K}'})$ with $\vec{K}' = \vec{k}_p + \vec{K}$,

and

$$K^2 = \left(\frac{\omega}{c}\right)^2\left[\left(\frac{k_p}{\omega/c}\right)^2 + \sin^2\theta - 2\frac{k_p}{\omega/c}\sin\theta \,\sin\phi\right].$$

This expression is the sum of the radiation from longitudinal and normal currents with the appropriate phases between these currents taken into account. $\sigma_\shortparallel$ and $\sigma_\perp$ are the conductivities parallel to and normal to the surface where we have allowed these to be different. $\omega_{\vec{k}_p}$ is the unperturbed plasmon energy ($\omega_{\vec{k}_p} = \omega$), $\omega_{\vec{K}'}$ is the unperturbed energy of a plasmon of momentum $\vec{K}'$. β is a slowly varying function expressing the variation of the scattering strength with wavelength. ω_{sp} is the surface-plasmon cutoff frequency.

This expression has been evaluated using the same autocorrelation function as for the scattered light of Sec. II A. The lifetime $1/\Gamma$ of the surface-plasmon states is treated as a parameter. A comparison with the experimentally observed anomaly is shown in Fig. 5, where $\Gamma/\omega_{\vec{k}_p}$ equals 0.32. The theoretical curve is moderately sensitive to Γ, a much sharper peak being predicted if the lifetime is longer. [6]

Plasmons excited by p-incident light will also radiate in the p direction, giving rise to the knee in Fig. 2. The calculation of its angular variation follows just as above, the only difference being that in the expression for P, $\cos^2\phi$ in the integral is replaced by $\sin^2\phi$. We find that the ratio of p-incident $- p$-scattered light to s-incident $- s$-scattered light for silver at 5500 Å is 3.2. The ratio varies only slowly with wavelength.

In the previous paper we estimated the total plasmon radiation when unpolarized light was incident onto the surface (Fig. 10 of paper I). Since the ratio of p-p to s-p light is approximately 3, the total radiation was taken to be two times the anomalous s-p radiation.

III. MODEL SURFACE REFLECTIVITY

As we described briefly in the previous paper, a model surface approach to the properties of rough surfaces appeared particularly useful, especially for short-range roughness. The existing solutions[2-4,7] are of restricted applicability, so we have taken a model which we can solve exactly, the

model surface consisting of spheres located above a smooth surface. The first-order term in the absorption for this model has been given by Berreman, but this neglects all the radiation effects. We use Mie's[8] solution, which is discussed in detail by van de Hulst[9] to calculate the scattering and extinction cross sections of isolated spheres, with the assumption that the mirror image does not distort the field around the spheres. The reflectivity of the model surface is given in terms of the forward- and backward-scattering cross sections of a simple sphere. By letting both the incident and the scattered fields reflect from the smooth surface, the boundary conditions on the smooth surface are fulfilled.

If a sphere is illuminated by a plane wave propagating along the z direction
$$u_0 = e^{-kz + i\omega t} \quad,$$
the scattered wave is a spherical outgoing wave
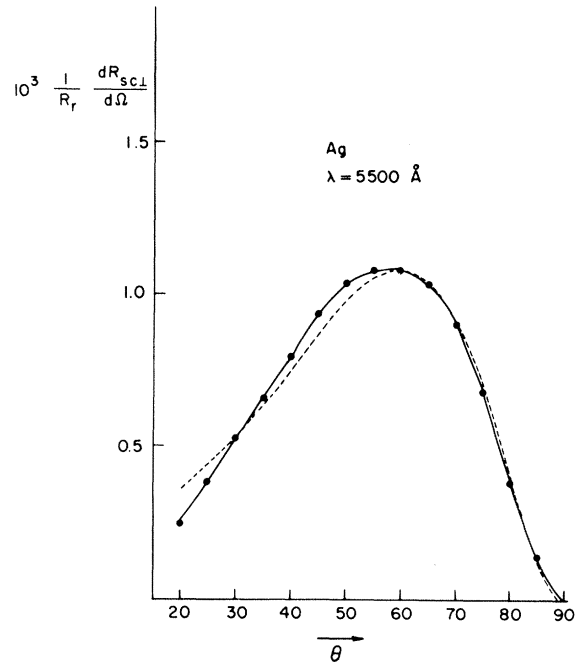$$u = S(\theta, \phi)e^{-ikr + i\omega t}/kr \quad.$$

FIG. 5. Angular distribution of relative anomalous scattering; solid line: experiment; dashed line: theory with $a = 1100$ Å and $\Gamma/\omega_{\vec{k}_p} = 0.32$.

With many scatterers lying in a plane, we can sum the scattering from all particles to find the fields in the forward direction

$$u = u_0 \left[1 - (2\pi/k^2)\rho S\,(0)\right]$$

and in the backscattered direction

$$u = -u_0 \,(2\pi/k^2)\rho S\,(180).$$

ρ is the number of spheres per unit area. Reflecting the forward wave from the smooth surface we find an amplitude reflection coefficient

$$r = r_0 \left[1 - p\left(\frac{Q\,(180)}{r_0} + 2Q(0) + r_0 Q(180)\right)\right]$$

(to first order in Q) from which we evaluate the decrease in reflectivity

$$\Delta R/R = 1 - |r/r_0|^2 \ .$$

We have introduced the cross sections $Q\,(0)$ and $Q\,(180)$ defined by

$$Q\,(\theta) = (4/x^2)\,S\,(\theta) \ .$$

r_0 is the smooth-surface amplitude reflection coefficient $(1 - \sqrt{\epsilon})/(1 + \sqrt{\epsilon})$, and $2p$ is the fraction of the area covered by the spheres. For small sphere sizes the scattering is symmetric, $Q\,(0) = Q\,(180)$, and the above expression reduces to

$$r = r_0 \left[1 - pQ\,(1 + r_0)^2/r_0\right] \ .$$

This can be interpreted as the extinction due to the spheres and their mirror images in the field $1 + r_0$ existing just above the surface. For very small sphere sizes such that $x = 2\pi a/\lambda \ll 1$ the term in Q is just the absorption from induced dipoles, $Q = i\frac{16}{3}\pi x\alpha$, α the sphere polarizability equal to $3\,(\epsilon - 1)/4\pi\,(\epsilon + 2)$, and we find the expression $\Delta R/R = 32p\;x\;\text{Im}\;1/(\epsilon + 2)$ for the relative decrease
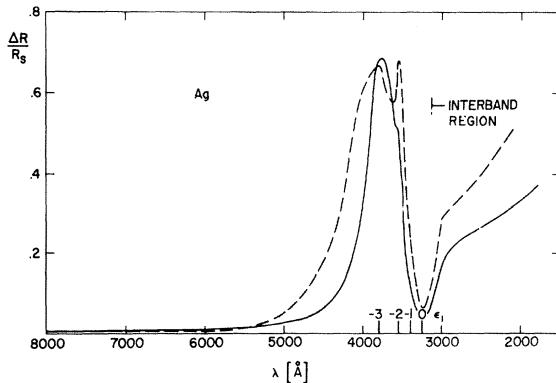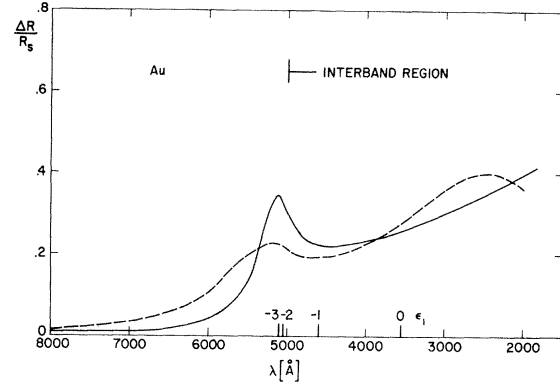

FIG. 7. Calculated relative decrease in reflectivity $\Delta R/R_s$ for gold plotted versus wavelength for two sphere sizes. Solid line: $a = 400\,\text{Å}$, $p = 0.06$; dashed line: $a = 800$ Å, $p = 0.03$.

in the reflectivity. This expression peaks where $\epsilon = -2$.

In this limit of small sphere size it is interesting to compare the reflectivity with the more realistic model of hemispheres on the surface used by Berreman. The polarizability of hemispheres in Berreman's model is found by truncating an infinite set of linear equations. With only the first equation he finds a polarizability $\alpha = 3(\epsilon - 1)/4\pi\,(\epsilon + \frac{1}{2})$ and a relative decrease in the reflectivity $\Delta R/R = 16p\;x\;\text{Im}\;1/(\epsilon + \frac{1}{2})$, which peaks at $\epsilon = -\frac{1}{2}$. Truncating at higher orders he finds a broad range of resonances lying in the range between $\epsilon = -4$ and $-\frac{1}{4}$. In this limit the behavior of the two models is thus similar, which gives us confidence that the extension of our solutions to include radiation effects is physically reasonable.

For larger sphere sizes, $Q(0)$ and $Q(180)$ and the fractional decrease in the reflectivity have
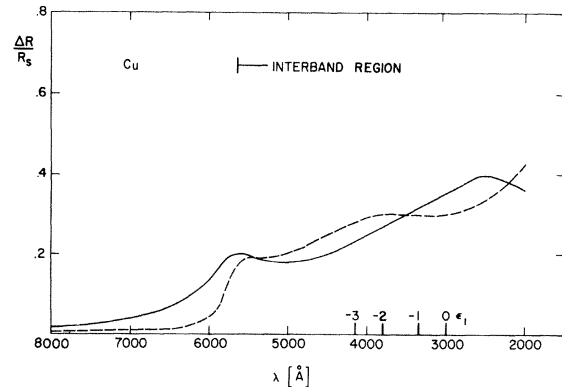

FIG. 6. Calculated relative decrease in reflectivity $\Delta R/R_s$ for silver plotted versus wavelength for two sphere sizes. Solid line: $a = 400\,\text{Å}$, $p = 0.045$; dashed line: $a = 500$ Å, $p = 0.065$.

FIG. 8. Calculated relative decrease in reflectivity $\Delta R/R_s$ for copper plotted versus wavelength for two sphere sizes. Solid line: $a = 400\,\text{Å}$, $p = 0.06$; dashed line: $a = 800$ Å, $p = 0.03$.
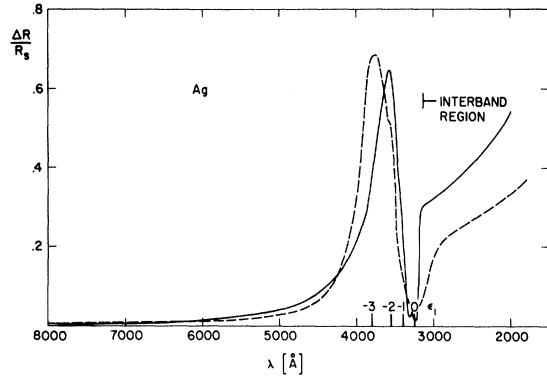
FIG. 9. Comparison of experiment and best theoretical fit. The relative decrease in reflectivity $\Delta R/R_s$ for silver; solid line: experiment, dashed line: theory with $a = 400$ Å, $p = 0.045$.
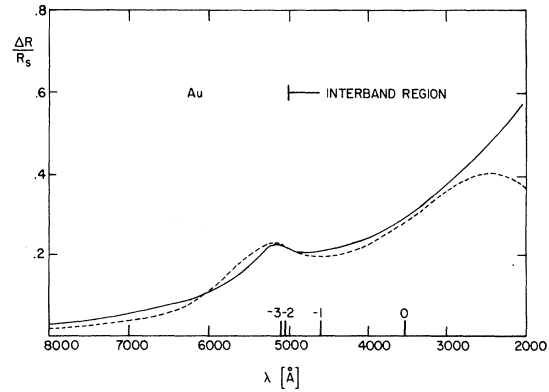

FIG. 10. Comparison of experiment and best theoretical fit. The relative decrease in reflectivity $\Delta R/R_s$ for gold; solid line: experiment, dashed line: theory with $a = 800$ Å, $p = 0.03$.

been evaluated keeping terms up to a_5 and b_5 in Mie's solution (see van de Hulst) – the a's and b's are essentially Bessel functions which were evaluated using their recurrence relations. The convergence was excellent even for 800-Å spheres, a_5 and b_5 being less than $\frac{1}{10}\%$ of the a_1 and b_1. Since x is typically greater than 1 for such spheres, an expansion in x is not useful here, and the beauty of Mie's solution is evident.

In Figs. 6–8, we show the relative changes in the reflectivity for two different sphere sizes calculated using the optical constants of bulk silver, gold, and copper. It can be seen that if the resonance falls in a free-electron region as for silver, the changes in reflectance are much more sensitive to the sphere size than if it falls in a damped region. In Figs. 9–11, we compare the calculated relative change in reflectivity with the experimental curves. a and p have been adjusted to give the best possible fit. The calculated curves show *all* the characteristic features of the observed fractional decrease in reflectivity. In Fig. 12, we show the fractional decrease in R for a Drude dielectric function.

The influence of the higher-order terms which are missing from Berreman's approach are seen most clearly if we plot the ratio of the two first terms in a series expansion in x for Q_{ext}. This is shown in Fig. 13, where we have plotted the first-order term Q_1 and the ratio of third- to first-order Q_3/Q_1 versus wavelength for silver spheres 400 Å in radius. This size extends the series expansion somewhat, but it is clearly seen that the higher-order term which contains the radiative fields is just as important as the first-order dipole absorption. The resonance in the third-order term is responsible for the sharp dip in $\Delta R/R$ observed for silver near the plasmon frequency, while the third-order term decreases the reflectivity at longer

wavelengths. Q_3 contains absorption as well as radiation, the latter coming from fields associated with currents around the surface of the sphere. The latter have a distribution characteristic magnetic dipole radiation, which increases Q (180) and decreases Q (0).

IV. CONCLUSIONS

These two approaches to the interaction of light with rough surfaces complement themselves well. The approach through currents handles those properties directly associated with induced currents, especially the angular distribution of the scattered light and the surface-plasmon radiation. The microscopic approach handles the rough-surface absorption most easily, but when solved in an exact fashion gives an excellent prediction for the total decrease in reflectance.
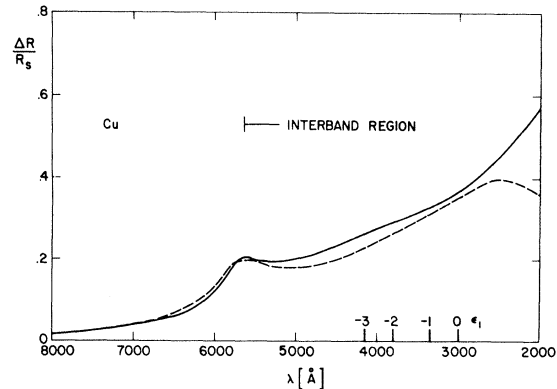

FIG. 11. Comparison of experiment and best theoretical fit. The relative decrease in the reflectivity $\Delta R/R_s$ for copper. Solid line: experiment; dashed line: theory with $a = 800$ Å, $p = 0.03$.
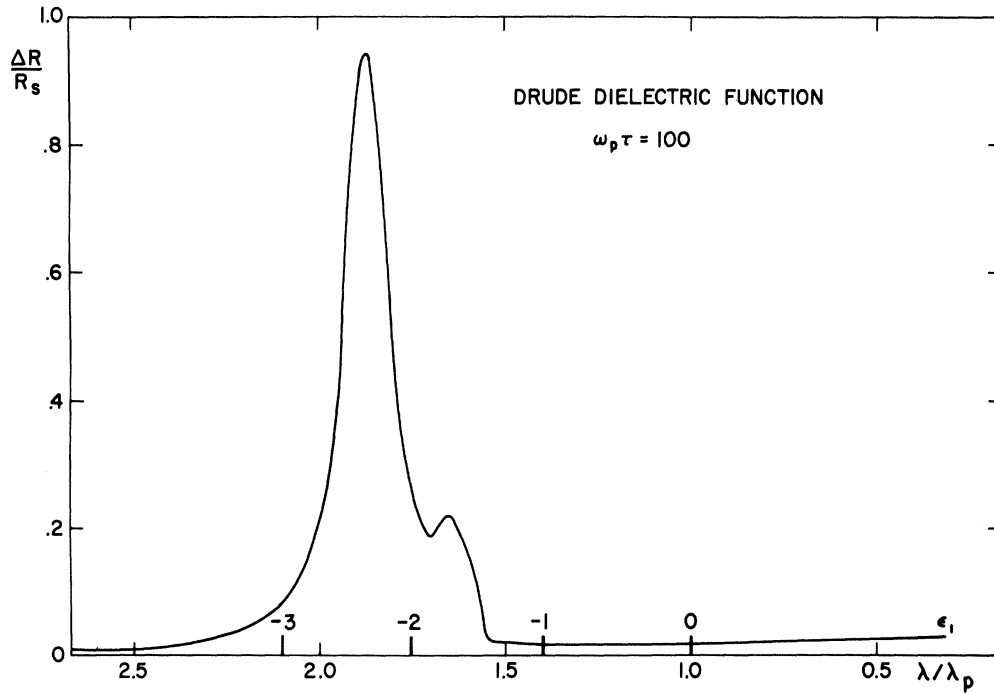
FIG. 12. Relative decrease in reflectivity $\Delta R/R_s$ plotted versus wavelength for a Drude dielectric function with parameters representative of aluminum and $a = 400$ Å, $p = 0.045$.
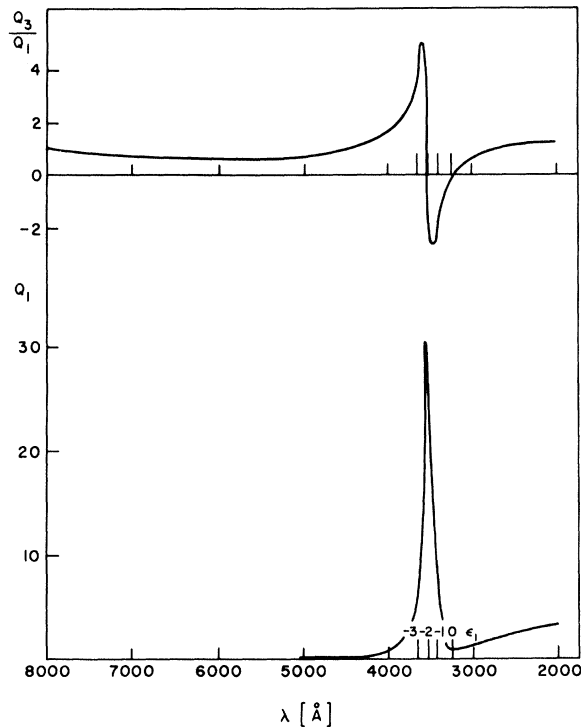

FIG. 13. Extinction cross section to first order in x, Q_1, and the ratio of the third-order term to the first-order term Q_1/Q_3 plotted versus wavelength for silver spheres of 400-Å radius.

APPENDIX: RADIATION FROM CURRENT SHEET

Consider a longitudinal current $\vec{j} = \vec{j}_{\vec{K}} \ e^{\ i\vec{K}\cdot\vec{r}}$ of thickness Δ with $\vec{j}_{\vec{K}}$ parallel to $\vec{K}$. The geometry is shown in Fig. 14. The vector potentials in all three regions satisfy the equation

$$\nabla^2 \vec{A}_{\vec{K}_n} - \frac{\epsilon_n}{c^2}\frac{\partial^2 \vec{A}_{\vec{K}_n}}{\partial t^2} = \frac{4\pi}{c}\ \vec{j}_n \qquad .$$

The subscript n representing the three regions, the fields are then determined by

$$\vec{B}_n = \nabla\times\vec{A}_{\vec{K}_n}, \quad \vec{E}_n = i\,(c/\omega)\,\nabla\times\vec{H}_n - (4\pi i/\omega)\ \vec{j}_n.$$

The solution for the differential equations for $\vec{A}_{\vec{K}}$ in regions 1 and 3 are plane waves with wave vector along the boundary $\vec{K}$, with amplitudes which we determine from the boundary conditions on the fields. In region 2, we must add a solution of the inhomogeneous equation to the plane-wave solutions:

$$\vec{A}_2 = -\frac{(4\pi/c)\vec{j}_{\vec{K}}\,e^{\ i(\vec{K}\vec{r}\,-\,\omega t)}}{(\omega/c)^2 - K^2} \qquad .$$

We determine $\vec{E}$ and $\vec{H}$ from the above equations. Using the boundary conditions for the fields at the two boundaries we obtain a set of linear equations which determine the unknown amplitudes $\vec{A}_{\vec{K}}$ in terms of the current amplitude $\vec{j}_{\vec{K}}$. The result for the vector potential above the surface is
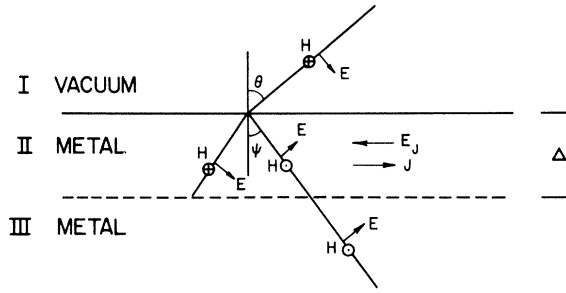
FIG. 14. Geometry for the radiation from a current sheet.

$$\vec{A}_{\vec{K}} = \frac{2\pi i\, \vec{j}_{\vec{K}}\Delta}{\omega\cos\Theta}\ \frac{2(\sqrt{\epsilon})\cos\psi}{(\sqrt{\epsilon})\cos\psi + \epsilon\cos\Theta}\ .$$

We assume the thickness of the current sheet is much smaller than the wavelengths in the media. $(\omega/c)\sin\theta = |\vec{K}|$ and ψ is the angle of propagation in the metal related to θ by Snell's Law.

In an analogous fashion we find for a transverse current lying in the surface

$$\vec{A}_{\vec{K}} = \frac{2\pi i\, \vec{j}_{\vec{K}}\Delta}{\omega\cos\theta}\ \frac{2\cos\theta}{(\sqrt{\epsilon})\cos\psi + \cos\theta}$$

and for a transverse current normal to the surface

$$\vec{A}_{\vec{K}} = \frac{2\pi i\, \vec{j}_{\vec{K}}\Delta}{\omega\cos\theta}\ \frac{2\cos\theta}{(\sqrt{\epsilon})\cos\psi + \epsilon\cos\theta}\ .$$

The fields above the surface are found from the vector potential, and using Poynting's vector $S = (c/8\pi)\ (E \times H^*)$ summing over all states reaching the detector we find a radiation per unit solid angle per unit area:

$$\frac{dI}{d\Omega} = \frac{c}{8\pi}\, k^4\cos^2\theta\ |\hat{n} \times \vec{A}_{\vec{K}}|^2\ .$$

$\hat{n}$ is the unit vector in the radiation direction.

---

[1]E. A. Stern, Phys. Rev. Letters **19**, 1321 (1967).

[2]D. W. Berreman, Phys. Rev. **163**, 855 (1967).

[3]V. Twersky, IRE Trans. Antennas Propagation AP-5, 81 (1957).

[4]H. Davis, Proc. Inst. Elec. Engrs. (London) **101**, 209 (1954); P. Beckman and A. Spizzichino *The Scattering of Electromagnetic Waves from Rough Surfaces* (Pergamon, New York, 1963).

[5]O. Hunderi and D. Beaglehole, Optics Commun. **1**, 101 (1969).

[6]In a recent report of a paper prior to publication, E. Kretschmann has used a somewhat similar approach to study the coherent radiation from surface plasmons; that is, radiation from surface plasmons which have not undergone additional scattering. In his solution the currents are taken to run along the boundary rather than in the metal, and this would lead to a different wavelength dependence if applied to our problem.

[7]P. A. Fedders, Phys. Rev. **165**, 580 (1968).

[8]G. Mie, Ann. Phys. (N. Y.) **25**, 377 (1908).

[9]H. C. van de Hulst, *Light Scattering by Small Particles* (Wiley, New York, 1957).